Published in : International Journal of Pharmaceutics (2022), 612 (121373)
DOI: 10.1016/j.ijpharm.2021.121373
Status : Postprint (Author's version)

EVALUATION OF DISTRIBUTIONAL HOMOGENEITY OF PHARMACEUTICAL FORMULATION USING LASER DIRECT INFRARED IMAGING

P.-Y. Sacré, M. Alaoui Mansouri, C. De Bleye, L. Coïc, Ph. Hubert, E. Ziemons

University of Liege (ULiege), CIRM, Vibra-Santé Hub, Department of Pharmacy, Laboratory of Pharmaceutical Analytical Chemistry, Liege, Belgium.

Keywords:

Laser direct infrared imaging; Raman imaging; Homogeneity; Vibrational spectroscopy; Distributional Homogeneity Index (DHI); Pharmaceutical formulations development

Abstract

The distributional homogeneity of chemicals is a key parameter of solid pharmaceutical formulations. Indeed, it may affect the efficacy of the drug and consequently its safety.

Chemical imaging offers a unique insight enabling the visualisation of the different constituents of a pharmaceutical tablet. It allows identifying ingredients poorly distributed offering the possibility to optimize the process parameters or to adapt characteristics of incoming raw materials to increase the final product quality.

Among the available chemical imaging tools, Raman imaging is one of the most widely used since it offers a high spatial resolution with well-resolved peaks resulting in a high spectral specificity. However, Raman imaging suffers from sample autofluorescence and long acquisition times. Recently commercialised, laser direct infrared reflectance imaging (LDIR) is a quantum cascade laser (QCL) based imaging technique that offers the opportunity to rapidly analyse samples.

In this study, a typical pharmaceutical formulation blend composed of two active pharmaceutical ingredients and three excipients was aliquoted at different mixing time points. The collected aliquots were tableted and analysed using both Raman and LDIR imaging. The distributional homogeneity indexes of one active ingredient image were then computed and compared. The results show that both techniques provided similar conclusions. However, the analysis times were drastically different. While Raman imaging required a total analysis time of 4 hours per tablet to obtain the distribution map of acetylsalicylic acid with a step size of 100 µm, it only took 7.5 minutes to achieve the same decision with LDIR for a single compound.

The results obtained in the present study show that LDIR is a promising technique for the analysis of pharmaceutical formulations and that it could be a valuable tool when developing new pharmaceutical formulations.

Published in : International Journal of Pharmaceutics (2022), 612 (121373)
DOI: 10.1016/j.ijpharm.2021.121373
Status : Postprint (Author's version)

Introduction

The homogeneity of distribution of active pharmaceutical ingredients (API) but also excipients is of utmost importance for the safety, efficacy, and final quality of solid pharmaceutical formulations. Therefore, the homogeneity of distribution of the ingredients is a key element to follow during the development of a new formulation. This homogeneity is generally assessed via chapter 2.9.40 "Uniformity of dosage units" of the European Pharmacopoeia requiring the dosage of the active ingredient in several units to compute the so-called acceptance value. However, this approach only provides insight into the inter-tablet homogeneity of the active ingredient. Therefore, the European Pharmacopoeia allows the pharmaceutical analyst to use chemical imaging (chapter 5.24 "chemical imaging") to explore the homogeneity of distribution of solid dosage forms ("intra-tablet" homogeneity) since it allows to assess the spatial distribution of API but also excipients (Sacré et al., 2015, 2014a) and is therefore recommended during the development of new formulations (Bøtker et al., 2020). Several techniques may be used to perform chemical imaging analysis of pharmaceutical formulations such as vibrational spectroscopy ((Sacré et al., 2014a), mass spectrometry (Belu et al., 2000; Earnshaw et al., 2010), SEM-EDX (Scoutaris et al., 2014) or UV spectroscopy (Klukkert et al., 2016). Among these, vibrational spectroscopy and more particularly which near-infrared (NIR) and Raman imaging (Gowen et al., 2008) are the most frequently used.

On the one hand, NIR imaging allows the fast analysis of several samples (Prats-Montalbán et al., 2012) but suffers from a low spatial resolution and a low spectral specificity (Carruthers et al., 2021). These two drawbacks imply the need for chemometrics and highly trained users to set up imaging experiments and complicate the analysis of finely dispersed pharmaceutical ingredients.

On the other hand, Raman imaging has a high spatial resolution (due to the shorter wavelength used) and a high spectral specificity enabling faster development of imaging experiments. However, Raman imaging suffers from sample autofluorescence, high risk of sample burning requiring the use of low laser power, and is usually performed in a point-mapping fashion implying long acquisition times (Stewart et al., 2012). Nevertheless, the hyperspectral data cube acquired enables the analysis of unknown formulations (Coic et al., 2019) making the development of a Raman imaging method quite straightforward.

Therefore, there is a need for fast and high-resolution imaging techniques enabling the generation of results within minutes. Non-linear Raman imaging techniques (coherent anti-stokes, CARS, or stimulated Raman spectroscopy, SRS) have recently been introduced with commercial equipment (Novakovic et al., 2017). These techniques, however, still suffer from sample autofluorescence, require highly trained staff to set up the imaging experiments and are yet very expensive.

The recent technological developments of quantum cascade lasers (QCL) (Bhargava, 2012) made them available in commercial spectroscopy equipment. Recently introduced, Laser Direct Infrared Reflectance (LDIR) imaging couples a QCL source with a single diode mercury

Published in : International Journal of Pharmaceutics (2022), 612 (121373)
DOI: 10.1016/j.ijpharm.2021.121373
Status : Postprint (Author's version)

cadmium telluride (MCT) detector. The device allows the imaging of samples at different spatial resolutions (1 to 40 µm) at relatively high speed. The images are acquired at a single wavelength between 975 and 1800 cm^{-1}. Therefore, to ensure the specificity of the imaging method, the sample constituents must be known a priori and must exhibit specific peaks corresponding to the studied compound without any interfering adjacent peak related to other compounds. The software allows both mappings of single peak intensities and classification methods. LDIR imaging has been successfully used to analyse microplastic pollution in water (Scircle et al., 2020) and to detect food raw materials adulteration (da Costa Filho et al., 2020).

The objective of this study was to evaluate the suitability of LDIR imaging to assess the homogeneity of distribution in a model pharmaceutical formulation. To achieve this goal, a pharmaceutical formulation containing two painkiller pharmaceutical ingredients and three common excipients was prepared. The blend of raw materials has been progressively mixed, and aliquots were taken at several time points. The different aliquots were tabletted and the whole tablet surface was analysed by LDIR and Raman imaging. The homogeneity of distribution of each compound was monitored and the results of both imaging techniques were compared. To objectivise the homogeneity of distribution, the distributional homogeneity index (DHI) approach has been chosen (Farkas et al., 2017; Sacré et al., 2014b; Wahl et al., 2017) and converted into homogeneity values. Finally, the blending endpoint and the homogeneity values were compared for both imaging techniques.

Material and methods

RAW MATERIALS

Most raw materials (paracetamol (Compap™ PVP3), lactose monohydrate, microcrystalline cellulose (Avicel® PH102) and magnesium stearate) were kindly provided by Galephar M/F (Marche-en-Famenne, Belgium). Acetylsalicylic acid (ASA) was purchased from Fagron Belgium NV (Nazareth, Belgium).

SAMPLE PREPARATION

A 50 g blend of powders was realized and placed in a mortar. The blend was composed of ASA (20% w/w), paracetamol (20% w/w), lactose (25% w/w), microcrystalline cellulose (30% w/w) and magnesium stearate (5% w/w). The powders were weighed and placed in the mortar in ascending order regarding the final proportion of the component in the blend.

The powders were mixed using a pestle and three aliquots of 200 mg were collected at different places in the mortar at each timepoint. A total of seven time points were analysed. Each time point corresponded to three turns of pestle at the exception of the first time point that was realized before any mixing, directly after the weighing of powders.

Published in : International Journal of Pharmaceutics (2022), 612 (121373)
DOI: 10.1016/j.ijpharm.2021.121373
Status : Postprint (Author's version)

The aliquots were placed into a 13 mm evacuable pellet die (Perkin Elmer, USA) and pressed at 1 T for 5 minutes. The final tablets were 2-3 mm thick and were glued (per time points) on a Menzel-Gläser microscope slide (Thermo Scientific, USA) using a cyanoacrylate glue.

The samples were directly analysed by LDIR after being pressed. The Raman experiments were conducted subsequently. The same total sample surface was analysed by both LDIR and Raman imaging. However, the final step size was slightly different (80 µm for LDIR and 100 µm for Raman microscopy) leading to a slightly different map size as explained below. A total of 21 tablets were analysed by both techniques (7 time points and 3 aliquots per time point)

LASER DIRECT INFRARED IMAGING (LDIR)

The laser direct infrared imaging analyses were performed using an Agilent's 8700 LDIR imaging system (Agilent Technologies, California, USA). The LDIR system relies on a quantum cascade laser (QCL) as the source and a thermoelectrically cooled single point Mercury Cadmium Telluride (MCT) as the detector. The spectra were recorded in the 975-1800 cm^{-1} spectral range with a data point spacing of 0.5 cm^{-1}. The direct reflectance module of the equipment was used in the present study. The 8700 LDIR produces a diffraction-limited spot on the sample. Depending on IR wavelength, it could be between 5.5 – 10 µm. The step size of the imaging experiments is adjustable between 1 and 40 µm.

LDIR METHOD DEVELOPMENT

The infrared chemical imaging methods were developed in the Clarity software (v.1.3.42).
The reference spectra have been recorded on small pellets (5 mm diameter) of pure material. A total of 100 direct reflectance spectra were recorded and averaged to constitute the reference spectrum of pure material, that was eventually added to the library.
Based on the acquired reference spectra, a single peak ratio analysis has been developed for each chemical present in the blend. This means that, for each chemical, two wavenumbers were chosen (peak and baseline position) based on visual inspection of the spectra at a spectral resolution of 8 cm^{-1}. The final pixel is the ratio of the baseline intensity and the peak intensity. Eventually, the five single peak methods were concatenated in a multipeak method. The whole tablet (13 mm diameter) was analysed at a step size of 40 µm (~330 x 330 pixels). The total analysis time for the multipeak analysis was 2.5 minutes. Autofocus of the system was performed on each tablet to avoid low-quality results due to differences in tablet thickness.
The output of the LDIR analysis is intensity images for each chemical. As these distribution maps cannot be exported for each chemical with the multipeak analysis, a single peak analysis has been performed for each chemical. These distribution maps were saved in the CSV format and transferred to Matlab for subsequent DHI/homogeneity analysis.

Published in : International Journal of Pharmaceutics (2022), 612 (121373)
DOI: 10.1016/j.ijpharm.2021.121373
Status : Postprint (Author's version)

CONFOCAL MICROSCOPY RAMAN IMAGING

Confocal microscopy Raman imaging experiments were performed on a Labram HR Evolution (Horiba Scientific) equipped with an EMCCD detector (1600×200-pixel sensor) (Andor Technology Ltd.), a Leica 50x Fluotar LWD objective and a 785 nm laser (XTRA II single frequency diode laser, Toptica Photonics AG) with a power reduced at 4.5 mW at a sample to avoid destruction by burning.

A circular point mapping experiment was performed with a step size of 100 µm (maps of 130 x 130 pixels) over the spectral range of 463 - 1853 cm^{-1}. The spectra were acquired with two accumulations of 0.1 sec exposure time and dispersed with a 300 gr/mm grating. The confocal slit hole was set at 200 µm and the electron-multiplying gain of the detector was set at 50.

DATA ANALYSIS

LDIR DATA ANALYSIS

The distribution maps of ASA were used to compute the homogeneity of distribution values. However, DHI cannot be computed on round images. Therefore, the biggest square inscribed in the circular distribution maps was extracted to compute DHI.

The maximum inscribed square map was computed using the formula:

$$S = \sqrt{\frac{d^2}{2}} \quad (1)$$

With S being the length of the square side (in pixels) and d being the diameter of the original distribution map. The obtained square distribution maps were of 233 x 233 pixels size.

The computation time of the DHI has an exponential relationship with the distribution map size. Therefore, to accelerate the DHI analysis, only one of each two pixels were kept reducing the distribution maps to a final size of 115 x 115 pixels. This reduced the DHI analysis time from 1244 min for 233 x 233 maps to ~7 min for 115 x 115 maps. The reduced maps were subsequently analyzed with the DHI algorithm. The reduction of the map also artificially increases the step size from 40 to 80 µm. This is done to lower the computation time of the homogeneity and to have more comparable results regarding the Raman experiments. Figure 1 illustrates the analysis process.

Published in : International Journal of Pharmaceutics (2022), 612 (121373)
DOI: 10.1016/j.ijpharm.2021.121373
Status : Postprint (Author's version)

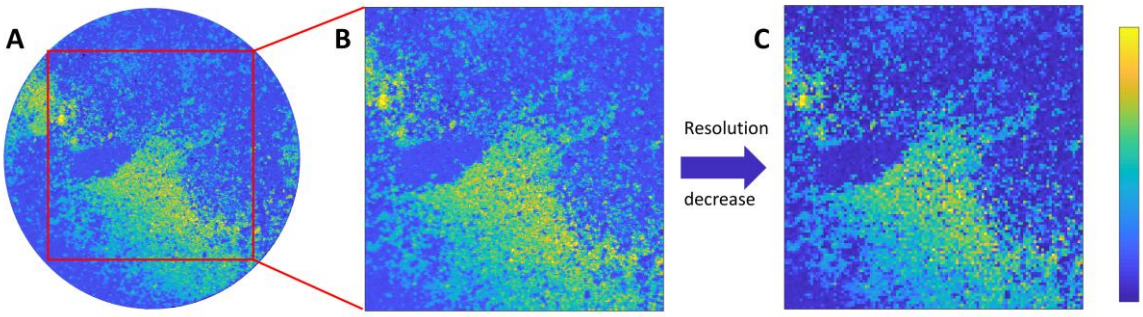

Figure 1: Extraction of the LDIR distribution map before the computation of the homogeneity. A: Distribution map of ASA obtained by single peak analysis; B: Maximum inscribed square map extracted from A (pixels size 230 x 230); C: Maximum inscribed square map keeping one each two pixels (pixels size 115 x115)

RAMAN DATA ANALYSIS

The raw Raman data were pre-processed using a Savitzky Golay smoothing (polynomial order: 2, window size: 7) followed by an asymmetric least squares (AsLS) baseline correction (p: 0.001, λ: 10^5) (Eilers, 2003; Savitzky and Golay, 1964).

The pre-processed data were eventually analysed using the MCR-ALS algorithm. Four components were resolved and the distribution map corresponding to ASA was used to compute the homogeneity of distribution value. The resolved loading exhibited a correlation coefficient above 0.9 with the ASA reference spectrum.

The maximum inscribed square map was computed using Equation 1. leading to a final square distribution map of 90 x 90 pixels (see Figure 2).

The pre-processing and MCR analysis were performed using the PLS Toolbox v. 8.9.2 and the MIA Toolbox v. 3.0.9 (Eigenvector Research Inc, USA) running in the Matlab R2018b (The Mathworks, USA) environment.

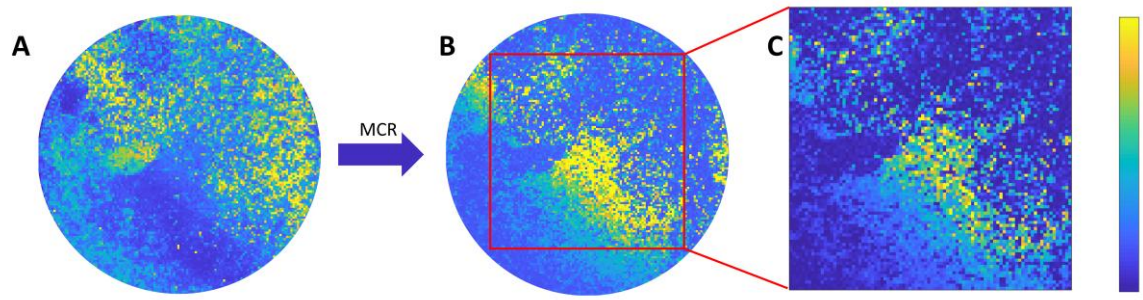

Figure 2: Extraction of the Raman imaging distribution map before the computation of the homogeneity. A: Average intensity Raman image; B: ASA distribution map resolved by MCR-ALS analysis of A; C: Maximum inscribed square map extracted from B (pixels size 90 x 90)

Published in : International Journal of Pharmaceutics (2022), 612 (121373)
DOI: 10.1016/j.ijpharm.2021.121373
Status : Postprint (Author's version)

DISTRIBUTIONAL HOMOGENEITY INDEX (DHI) ANALYSIS

The analysed tablet surface was the same for both Raman and LDIR imaging. Only the spatial resolution was different (step size of ~80 µm for LDIR and ~100 µm for Raman imaging). The square distribution maps were analysed with the DHI algorithm (Sacré et al., 2014b) with a number of simulations n=100.

The DHI analysis comprises several steps among which the distribution map is first sampled by a Continuous-Level Moving Block (CLMB). For each macropixel size, the standard deviation of the macropixel value is computed. Then, the standard deviation is plotted against the macropixel size to obtain the so-called "homogeneity curve". Once the homogeneity curve is obtained for the studied distribution map, the map is randomized and the homogeneity curve of the random map is computed. The DHI value is obtained by the ratio of the area under the homogeneity curve (AUC) of the studied map and the area under the homogeneity curve of the randomized map. Because of the randomization step, many simulations are necessary to compute a mean DHI value assorted with a standard deviation value.

To ease the interpretation of DHI values, the latter were converted into homogeneity values expressed as a percentage of homogeneity. The conversion into homogeneity values was realized using simulated maps (of pixel size 90 x 90 and 115 x 115 for Raman and LDIR data respectively) with increasing levels of homogeneity between 10 and 90 %. Three maps were simulated per level of homogeneity and their average DHI value was computed with a number of simulations set to n=100. The ordinary least squares (OLS) regression coefficients were computed, and the coefficients of determination were above 0.99 for each map size. Figure S1 shows the OLS regression lines for the simulated maps.

HARDWARE DESCRIPTION:

All computations were performed on a portable computer with the following specifications:

- Win10 Professional 64-bit
- Intel i5-6440HQ CPU 2.6 GHz Processor
- 1TB SSD
- 16GB RAM
- AMD Radeon R7 M370 graphics card

Results and discussion

LDIR ANALYSIS

Once the imaging method is developed, analysing samples with the LDIR system is very fast and straightforward. However, the development of the method may be a difficult and tedious task. Indeed, the analyst can choose different analyses options (single peak ratio with one or two baseline points or classification analysis) but all these options are based on the selection of

Published in : International Journal of Pharmaceutics (2022), 612 (121373)
DOI: 10.1016/j.ijpharm.2021.121373
Status : Postprint (Author's version)

a single wavelength (plus one or two baseline points) to represent the compound of interest. Therefore, the analysis of complex samples (more than 2 or 3 compounds) is dependent on the spectral signature and the possible overlapping of the individual spectral signals. This task is also complicated by the shape of direct reflectance IR signals exhibiting larger and less resolved peaks compared to Raman or transmission IR spectra because of the superposition of diffuse and specular reflected light (Fringeli, 1999). Figure 3 shows the LDIR spectra acquired on pure compound pellets.

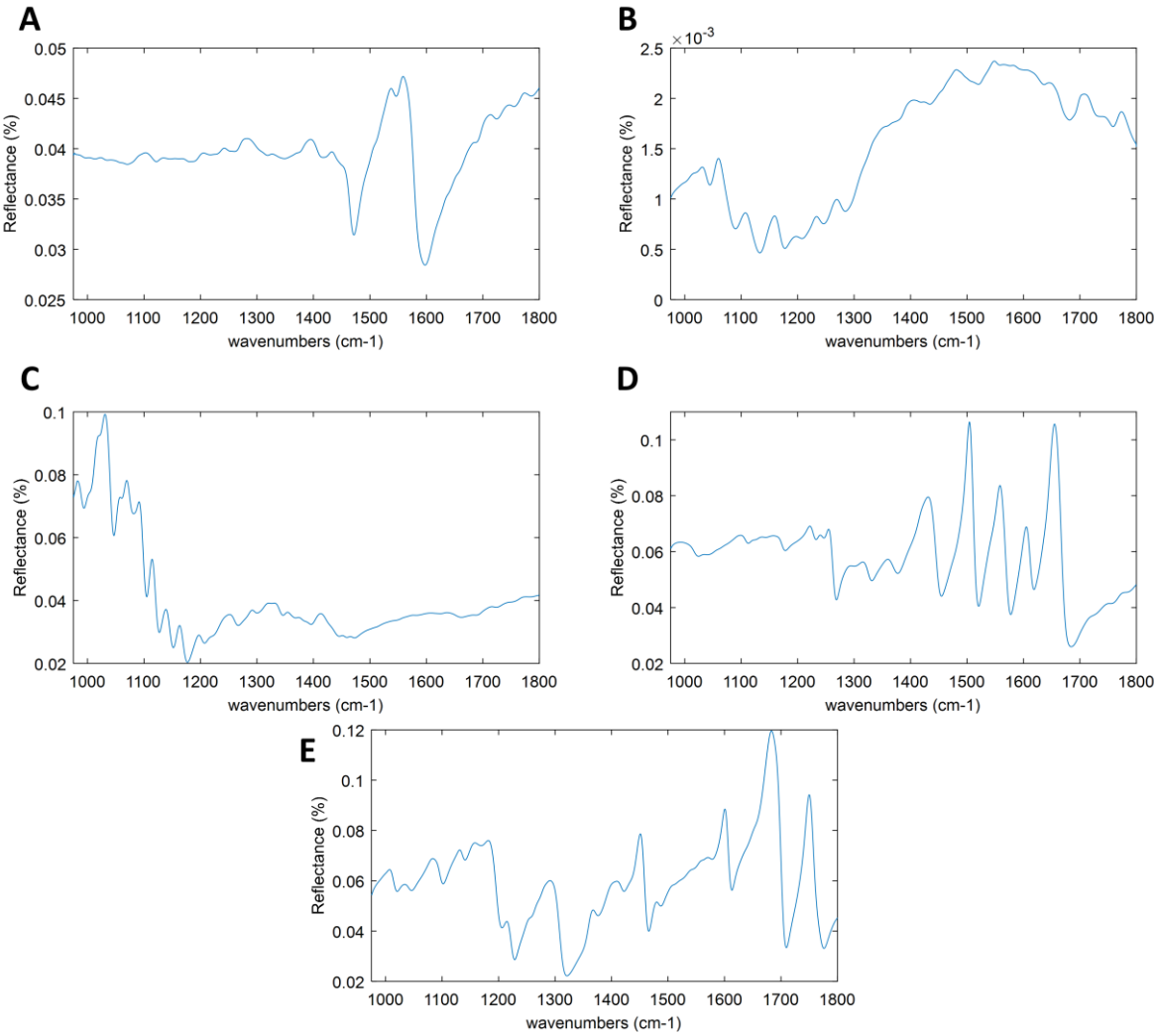

Figure 3: LDIR spectra of the pure compounds of the pharmaceutical blend: Magnesium stearate (A), microcrystalline cellulose (B), lactose (C), paracetamol (D) and acetylsalicylic acid (E)

In the present work, it was decided to build single peak ratio (with one baseline point) analyses for each compound. These single peak ratio methods were eventually combined as a "multipeak analysis". This choice was guided by the will of obtaining a distribution map of intensity values for each compound that is more realistic. Indeed, depending on the spatial

Published in : International Journal of Pharmaceutics (2022), 612 (121373)
DOI: 10.1016/j.ijpharm.2021.121373
Status : Postprint (Author's version)

resolution (step size), the spot size of the system and the particle size of the powders analysed, it is very likely that more than one compound is present in a single pixel, the measured spectrum being the weighted sum of the individual compound spectra. The classification method automatically assigns a single compound for each analysed pixel based on a predefined classification rule. The classification method works by comparing ratios of peaks, and the individual pixel gradient or brightness represents the normalized value of the ratio for the classified component. This provides some texture to the image to present a more 'natural' feel and gives the user an idea of where the ratio is strongest. Table 1 listed the wavelength values for each peak and baseline used in the single peak ratio analyses. These peak and baseline wavelengths are presented on the corresponding spectra in figures S2 – S6.

Once the method is developed, the analysis time is very short since it took 2.5 min between the start of the imaging experiment and the display of the results (31 sec for each single peak analysis). The result of the analysis is the distribution map of the five components in the tablet. Figure 4 shows the distribution maps obtained with the LDIR system for each of the 21 tablets analysed (three tablets per time point and seven time points analysed). Shadows may be observed on some tablets (especially on tablets 1 and 3 of time point 4). These shadows are linked to small differences between the tablet surface and the light (out-of-focus) coming from the fact that some tablets were not lying perfectly flat on the microscope slide. This information is available in the single and multipeaks analysis because the analysis result is an intensity value for each compound in each pixel. This would have been avoided if a classification analysis model is used since the output is a categorical response. Another option, that is now commonly available on most Raman imaging systems is a topographic mapping of the sample before the Raman imaging analysis allowing an automatic adjustment of the collection optics distance to the sample keeping it constant throughout the analysis.

A straightforward visual inspection of the images shows that the different compounds are more and more homogeneously distributed as the mixing time increases. Magnesium stearate is only visible in the first time points T_0 and T_1. Lactose and microcrystalline cellulose are not observed in each tablet at the first time points because of the inhomogeneous distribution of the powders at the beginning of the mixing process. The different components are progressively blended, and their distribution becomes more and more homogeneous. However, it is difficult to visually assess the endpoint of the blending process. Therefore, a DHI analysis of the distribution maps has been realized to objectify the homogeneity of distribution (Sacré et al., 2014b).

Another question that arose from the development of the LDIR model was the confidence that we may have in the distribution maps obtained using a univariate analysis of pharmaceutical tablets. Therefore, we performed the same analyses using a Raman confocal microscope to compare the results obtained with both systems.

Published in : International Journal of Pharmaceutics (2022), 612 (121373)
DOI: 10.1016/j.ijpharm.2021.121373
Status : Postprint (Author's version)

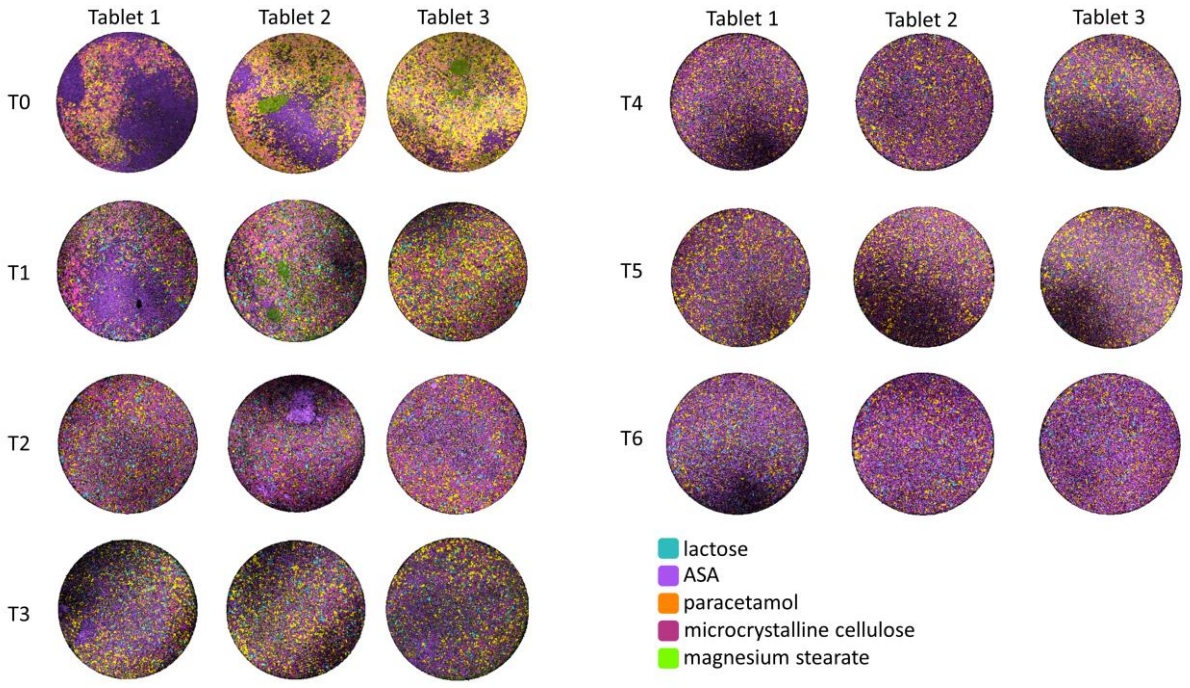

Figure 4: Results of the LDIR multipeaks imaging analysis of the tablets. Three tablets are presented for each timepoint (T_0 – T_6).

RAMAN IMAGING ANALYSIS

The tablets previously analysed by LDIR were eventually analysed with a Raman confocal microscope. Compared to the LDIR system, the setup of the Raman imaging analyses is very fast since the data analysis is realised afterwards. To avoid any burning of the tablet, the laser power was reduced to 4.5 mW on sample. This leads to an increase in the acquisition time to get a satisfying signal over noise ratio, increasing the overall analysis time to 183 min per tablet. To this time, one must still add the data processing time (~1h) leading to a total analysis time of about 4 hours (~240 min) compared to the 7.5 min of LDIR (~0.5 min for the LDIR analysis and ~7 min for the DHI computation).

MCR-ALS has been used with a various number of components to extract. Three components were selected to obtain the distribution maps of the active pharmaceutical ingredients (ASA, paracetamol). To resolve the minor compounds (microcrystalline cellulose, lactose, and magnesium stearate), an MCR of 9 components was necessary. The quality of the resolution was assessed by computing the correlation coefficient between the resolved spectrum and the reference spectrum. A correlation coefficient above 0.9 was found satisfactory since a correlation coefficient of 1 describes a perfect match. Although present in each tablet, magnesium stearate was not resolved in several tablets of timepoints T_4, T_5 and T_6 because of the intimate mixture of the blend and its low concentration.

The resolved distribution maps of the Raman experiments were visually compared to the LDIR individual distribution maps (Figure 5). This comparison was performed at T_0 since it is the time point with the highest inhomogeneity showing clear patterns. It was found that the LDIR

Published in : International Journal of Pharmaceutics (2022), 612 (121373)
DOI: 10.1016/j.ijpharm.2021.121373
Status : Postprint (Author's version)

distribution maps were reasonably following the Raman imaging results confirming that the developed method was able to monitor the distribution of each compound. Nevertheless, some discrepancies may be observed between the two methods (e.g. ASA in tablet 1). These discrepancies may come from the fact that the imaging setups are different along with different collection optics and the underlying physical mechanisms are also different (absorption vs scattering). In addition to these technical differences, the data analysis is completely different (peak ratio for LDIR vs multivariate data analysis for Raman).

Therefore, these differences will also be present in the DHI analysis.

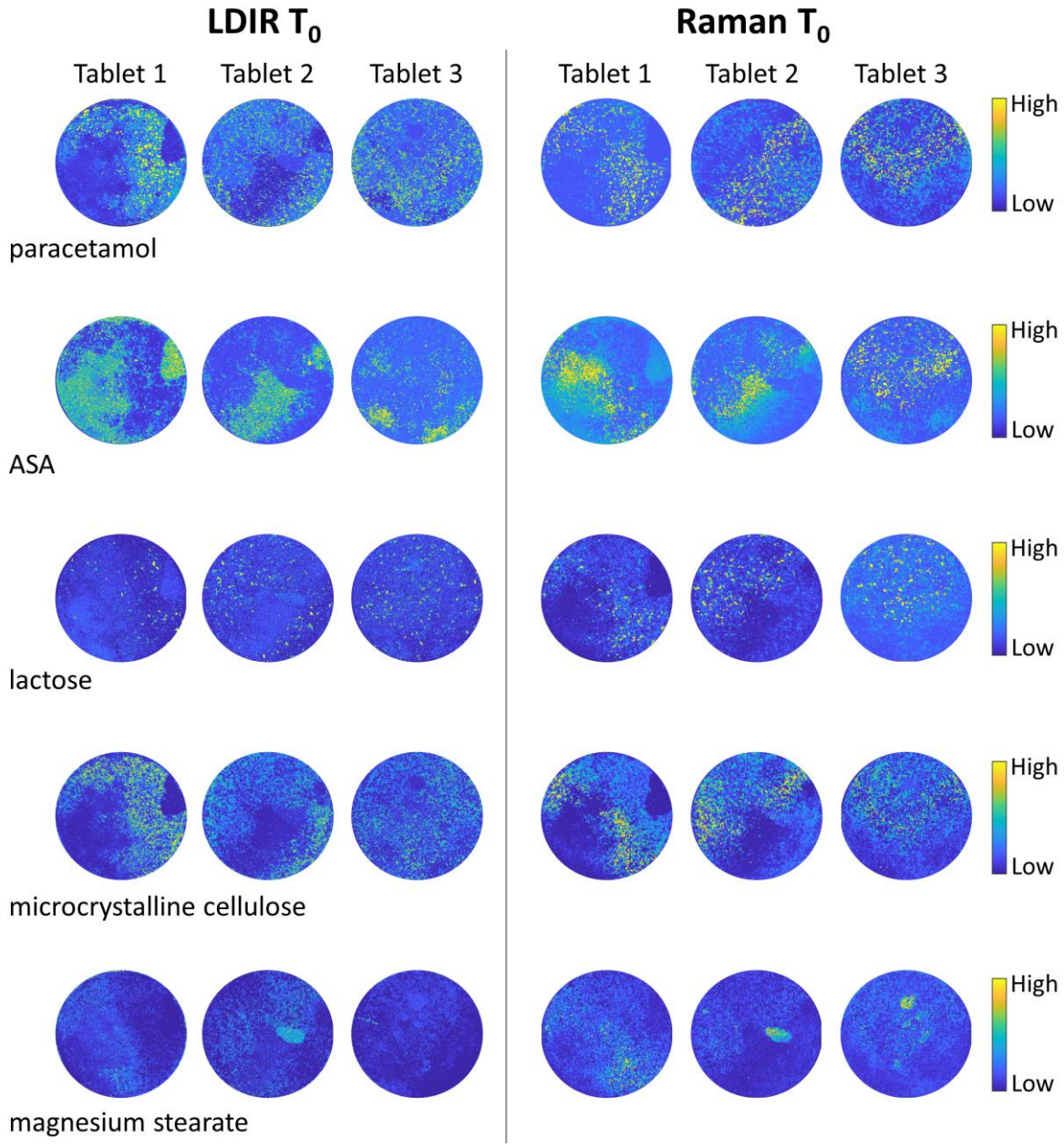

Figure 5: Comparison of the distribution maps obtained for each compound with LDIR (single peak ratio imaging analysis) and Raman imaging (after MCR-ALS analysis) of the tablets per timepoint.

Published in : International Journal of Pharmaceutics (2022), 612 (121373)
DOI: 10.1016/j.ijpharm.2021.121373
Status : Postprint (Author's version)

HOMOGENEITY OF TABLETS

The homogeneity results of individual tablets are presented in supplementary table ST1.

Figure 6 summarizes the results of the homogeneity computations at each time point for both Raman and LDIR experiments. The error bars were computed as the standard error (SE) using the following formula:

$$SE = \frac{\sigma_i}{\sqrt{n_i}}$$

Where σ_i is the standard deviation of the computed homogeneity at timepoint i and is the number of replicates at timepoint i.

For the first three time points, there is a low average homogeneity of distribution among single tablets, but, above all, a high inhomogeneity between tablets. This was expected from the visual inspection of the LDIR multipeaks images (see Figure 4). However, the visual appreciation is now objectivised through the computation of homogeneity. The blend appears to be homogeneous at time point 4 with an almost constant average homogeneity of ~90 % for LDIR and ~80 % for Raman experiments, respectively. The standard errors also become very small at this stage. The homogeneity computed from the Raman data appears to be slightly lower than the one from the LDIR experiments. This might come from the "shadow effect" observed due to the slightly non-flat surface of the tablets but also from the lower spatial resolution of the Raman experiments. Nevertheless, the endpoint of the blending is easily found and is coherent with the LDIR experiments.

Published in : International Journal of Pharmaceutics (2022), 612 (121373)
DOI: 10.1016/j.ijpharm.2021.121373
Status : Postprint (Author's version)

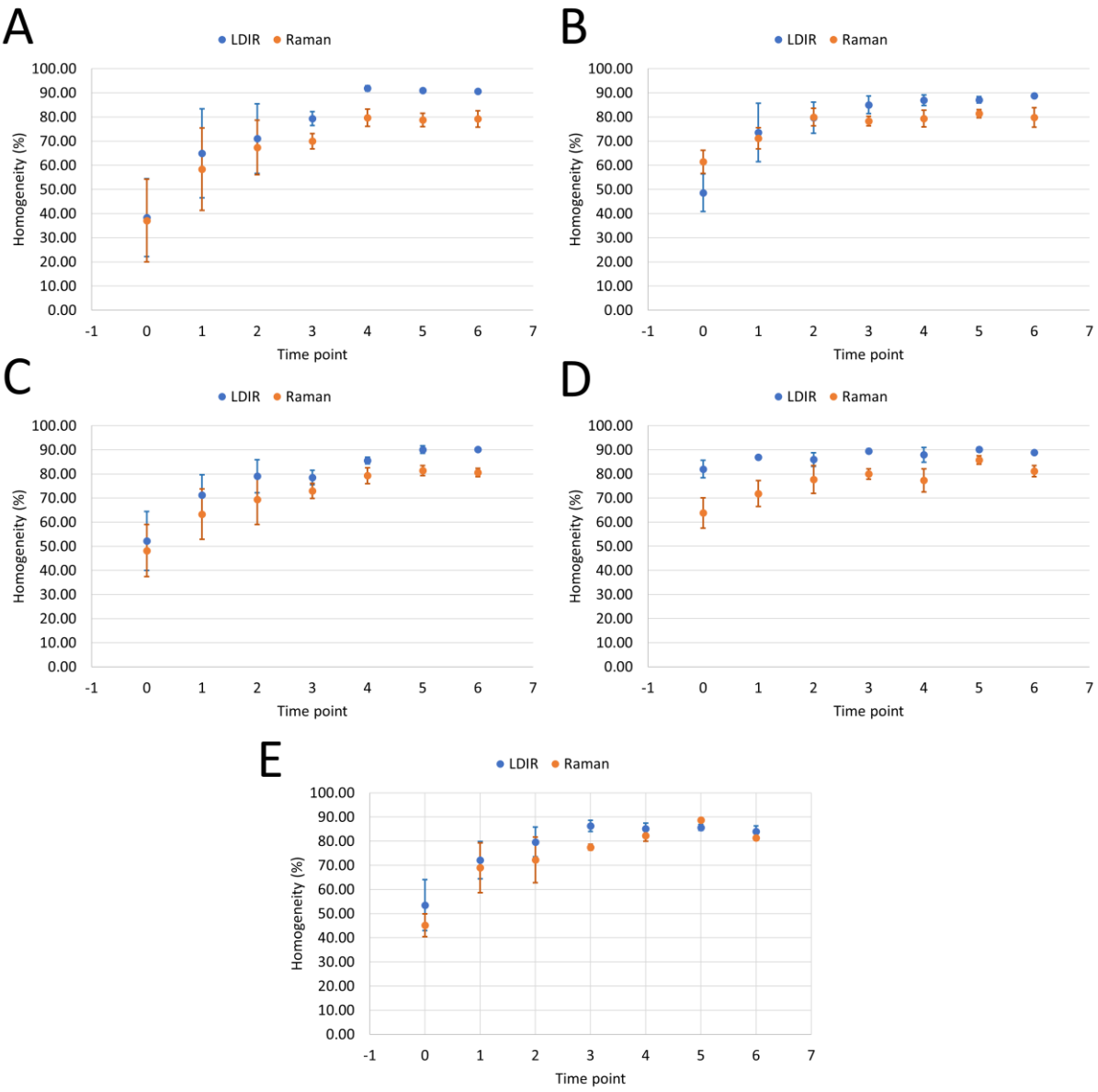

Figure 6: Average homogeneity computed for each timepoint for LDIR and Raman distribution maps of A) ASA, B) Paracetamol, C) Microcrystalline cellulose, D) Lactose, E) Magnesium stearate.

Conclusion

Distributional homogeneity of compounds in a pharmaceutical formulation is a key parameter to be monitored since it may affect the efficacy and safety of the formulation.

Usually, this parameter is estimated by dosing the active pharmaceutical ingredient in several tablets and computing the well-known acceptance value following the pharmacopoeia rules.

Published in : International Journal of Pharmaceutics (2022), 612 (121373)
DOI: 10.1016/j.ijpharm.2021.121373
Status : Postprint (Author's version)

However, the acceptance value only informs about the inter-tablet homogeneity of the active ingredient. No information is provided regarding the intra-tablet API distribution or the distribution of excipients. This information is very important when developing a new formulation as it may influence the process parameters or properties of entry raw materials (particle size, etc.). A unique tool that provides this information is the chemical imaging technology allowing the pharmaceutical analyst to visualise the distribution of the main compounds at the surface of the tablet.

Nevertheless, when the method is successfully developed, results are obtained in a handful of seconds. Therefore, it is possible to analyse several tablets and get a unique insight into "intra-tablet" homogeneity and "inter-tablet" homogeneity. The latter is difficult to obtain with Raman imaging because of the long acquisition times making the analysis of several tablets difficult.

Based on the presented results, LDIR seems to be a very promising tool for the analysis of the spatial distribution of chemicals in a pharmaceutical formulation. This might be very useful in routine analysis of pharmaceutical blends as quality control of the produced tablets but most of all during the development of new formulations. Indeed, when a new pharmaceutical formulation is developed, the choice of excipients, raw materials particle size or even the process parameters may greatly influence the homogeneity of distribution of chemicals (Chavez et al., 2015) and, consequently, the efficacy and safety of the formulation. Usually, this homogeneity is assessed through liquid chromatography analysis of the content of API of the different formulations. However, this conventional workflow is tedious, needs a lot of organic solvents and lab work and it does neither provide any insight into the "intra-tablet" homogeneity nor information regarding excipients. These two last points may only be assessed using hyperspectral imaging such as NIR or Raman imaging. However, NIR imaging suffers from a low spatial resolution and high penetration depth (hundreds of micrometres compared to a maximum of 15-20 µm for both LDIR and Raman) leading to blurred results (Carruthers et al., 2021). Raman imaging is relatively slow making the analysis of several tablets at a high spatial resolution hardly compatible with the industrial needs and it suffers from autofluorescence of chemicals (such as cellulose derivatives that are often used as excipients).

LDIR, on its side, suffers from the difficulty to setup methods when the sample is complex and does not allow a straightforward selection of unique peaks attributable to specific compounds since it images the intensity of IR reflectance at unique wavenumbers.

On the one hand, Raman spectroscopy imaging systems collecting data over a spectral range at each measured pixel have a high spectral specificity leading to a higher versatility allowing the analysis of unknown formulations or the analysis of spectra modified by the manufacturing process (chemical interactions, solid-state modifications etc.). However, this is at the cost of long analysis times. On the other hand, once the method is developed and validated or "confirmed" by another technique, LDIR enables the analysis of tablets at high speed (~31 sec per compound per tablet) which is valuable and constitutes a plus-value during the development of a new pharmaceutical formulation for routine quality control analyses.

Published in : International Journal of Pharmaceutics (2022), 612 (121373)
DOI: 10.1016/j.ijpharm.2021.121373
Status : Postprint (Author's version)

Acknowledgements

Research grants from the Walloon Region of Belgium and the EU Commission (project FEDER-PHARE) to L. Coïc are gratefully acknowledged.

FNRS and FWO through the Chimic EOS project are also acknowledged (P-Y Sacré).

Agilent is acknowledged for the lend of the LDIR system used in the present study.

References

Belu, A.M., Davies, M.C., Newton, J.M., Patel, N., 2000. TOF-SIMS characterization and imaging of controlled-release drug delivery systems. Anal. Chem. 72, 5625–5638. https://doi.org/10.1021/ac000450+

Bhargava, R., 2012. Infrared Spectroscopic Imaging: The Next Generation. Appl. Spectrosc. 66, 1091–1120. https://doi.org/10.1366/12-06801

Bøtker, J., Wu, J.X., Rantanen, J., 2020. Hyperspectral imaging as a part of pharmaceutical product design, in: Data Handling in Science and Technology. Elsevier Ltd, pp. 567–581. https://doi.org/10.1016/B978-0-444-63977-6.00022-5

Carruthers, H., Clark, D., Clarke, F., Faulds, K., Graham, D., 2021. Comparison of Raman and Near-Infrared Chemical Mapping for the Analysis of Pharmaceutical Tablets. Appl. Spectrosc. 75, 178–188. https://doi.org/10.1177/0003702820952440

Chavez, P.-F., Lebrun, P., Sacré, P.-Y., De Bleye, C., Netchacovitch, L., Cuypers, S., Mantanus, J., Motte, H., Schubert, M., Evrard, B., Hubert, P., Ziemons, E., 2015. Optimization of a pharmaceutical tablet formulation based on a design space approach and using vibrational spectroscopy as PAT tool. Int. J. Pharm. 486, 13–20. https://doi.org/10.1016/j.ijpharm.2015.03.025

Coic, L., Sacré, P.-Y., Dispas, A., Sakira, A.K., Fillet, M., Marini, R.D., Hubert, P., Ziemons, E., 2019. Comparison of hyperspectral imaging techniques for the elucidation of falsified medicines composition. Talanta 198, 457–463. https://doi.org/10.1016/j.talanta.2019.02.032

da Costa Filho, P.A., Cobuccio, L., Mainali, D., Rault, M., Cavin, C., 2020. Rapid analysis of food raw materials adulteration using laser direct infrared spectroscopy and imaging. Food Control 113, 107114. https://doi.org/10.1016/j.foodcont.2020.107114

Earnshaw, C.J., Carolan, V.A., Richards, D.S., Clench, M.R., 2010. Direct analysis of pharmaceutical tablet formulations using matrix-assisted laser desorption/ionisation mass spectrometry imaging. Rapid Commun. Mass Spectrom. 24, 1665–1672. https://doi.org/10.1002/rcm.4525

Eilers, P.H.C., 2003. A Perfect Smoother. Anal. Chem. 75, 3631–3636. https://doi.org/10.1021/ac034173t

Published in : International Journal of Pharmaceutics (2022), 612 (121373)
DOI: 10.1016/j.ijpharm.2021.121373
Status : Postprint (Author's version)

Farkas, A., Nagy, B., Marosi, G., 2017. Quantitative Evaluation of Drug Distribution in Tablets of Various Structures via Raman Mapping. Period. Polytech. Chem. Eng. 1–7.

Fringeli, U.P., 1999. ATR and Reflectance IR Spectroscopy, Applications*, in: Encyclopedia of Spectroscopy and Spectrometry. Elsevier, pp. 94–109. https://doi.org/10.1016/B978-0-12-374413-5.00104-4

Gowen, A.A., O'Donnell, C.P., Cullen, P.J., Bell, S.E., 2008. Recent applications of Chemical Imaging to pharmaceutical process monitoring and quality control. Eur J Pharm Biopharm 69, 10–22. https://doi.org/10.1016/j.ejpb.2007.10.013

Klukkert, M., Wu, J.X., Rantanen, J., Carstensen, J.M., Rades, T., Leopold, C.S., 2016. Multispectral UV imaging for fast and non-destructive quality control of chemical and physical tablet attributes. Eur. J. Pharm. Sci. 90, 85–95. https://doi.org/10.1016/j.ejps.2015.12.004

Novakovic, D., Saarinen, J., Rojalin, T., Antikainen, O., Fraser-Miller, S.J., Laaksonen, T., Peltonen, L., Isomäki, A., Strachan, C.J., 2017. Multimodal Nonlinear Optical Imaging for Sensitive Detection of Multiple Pharmaceutical Solid-State Forms and Surface Transformations. Anal. Chem. 89, 11460–11467. https://doi.org/10.1021/acs.analchem.7b02639

Prats-Montalbán, J.M., Jerez-Rozo, J.I., Romañach, R.J., Ferrer, A., 2012. MIA and NIR Chemical Imaging for pharmaceutical product characterization. Chemom. Intell. Lab. Syst. 117, 240–249. https://doi.org/10.1016/j.chemolab.2012.04.002

Sacré, P.-Y., De Bleye, C., Chavez, P.-F., Netchacovitch, L., Hubert, P., Ziemons, E., 2014a. Data processing of vibrational chemical imaging for pharmaceutical applications. J. Pharm. Biomed. Anal. 101, 123–140. https://doi.org/10.1016/j.jpba.2014.04.012

Sacré, P.-Y., Lebrun, P., Chavez, P.-F., De Bleye, C., Netchacovitch, L., Rozet, E., Klinkenberg, R., Streel, B., Hubert, P., Ziemons, E., 2014b. A new criterion to assess distributional homogeneity in hyperspectral images of solid pharmaceutical dosage forms. Anal. Chim. Acta 818, 7–14. https://doi.org/10.1016/j.aca.2014.02.014

Sacré, P.-Y., Netchacovitch, L., De Bleye, C., Chavez, P.-F., Servais, C., Klinkenberg, R., Streel, B., Hubert, P., Ziemons, E., 2015. Thorough characterization of a Self-Emulsifying Drug Delivery System with Raman hyperspectral imaging: A case study. Int. J. Pharm. 484, 85–94. https://doi.org/10.1016/j.ijpharm.2015.02.052

Savitzky, A., Golay, M.J.E., 1964. Smoothing and Differentiation of Data by Simplified Least Squares Procedures. Anal Chem 36, 1627–1639. https://doi.org/10.1021/ac60214a047

Scircle, A., Cizdziel, J. V., Tisinger, L., Anumol, T., Robey, D., 2020. Occurrence of Microplastic Pollution at Oyster Reefs and Other Coastal Sites in the Mississippi Sound, USA: Impacts of Freshwater Inflows from Flooding. Toxics 8, 35. https://doi.org/10.3390/toxics8020035

Scoutaris, N., Vithani, K., Slipper, I., Chowdhry, B., Douroumis, D., 2014. SEM/EDX and confocal Raman microscopy as complementary tools for the characterization of pharmaceutical tablets. Int. J. Pharm. 470, 88–98. https://doi.org/10.1016/j.ijpharm.2014.05.007

Published in : International Journal of Pharmaceutics (2022), 612 (121373)
DOI: 10.1016/j.ijpharm.2021.121373
Status : Postprint (Author's version)

Stewart, S., Priore, R.J., Nelson, M.P., Treado, P.J., 2012. Raman imaging. Annu Rev Anal Chem (Palo Alto Calif) 5, 337–360. https://doi.org/10.1146/annurev-anchem-062011-143152

Wahl, P.R., Pucher, I., Scheibelhofer, O., Kerschhaggl, M., Sacher, S., Khinast, J.G., 2017. Continuous monitoring of API content, API distribution and crushing strength after tableting via near-infrared chemical imaging. Int. J. Pharm. 518, 130–137. https://doi.org/10.1016/J.IJPHARM.2016.12.003